Linearity Improvement of Microwave FM Oscillators by Harmonic Tuning

GYÖRGY G. ENDERSZ

Abstract—**A new linearizing method for microwave communication FM oscillators is presented. As a linearizing mechanism the frequency perturbation caused by tuned harmonic(s) is utilized. Analytical formulation of linearity requirements for the general case are given and explicit relations are delivered for the second harmonic-tuned FM oscillator. Linearity and noise loading results are shown, obtained with an experimental 250-mW *X* band Gunn diode FM oscillator and satisfying CCIR linearity and noise loading requirements for broad-band microwave radio links.**

NOMENCLATURE

A	Capacitance ratio.
a_n	Amplitude of the nth harmonic.
C	Capacitance.
f	Frequency.
f'	Normalized frequency.
f_0	Undisturbed resonator frequency.
Δf	Small change of frequency.
f_a	Frequency perturbation caused by harmonics.
f_m	Frequency of varactor tuned resonator.
f_{mr}	Output frequency of FM oscillator.
G	Conductance.
$H(j\omega)$	Transfer function of linear passive network.
I	Current amplitude.
k	Circuit constant.
L	Inductance.
N	Nonlinearity.
Q	Quality factor of resonant circuit.
S	Derivative of frequency characteristic (modulation sensitivity).
S'	Normalized derivative.
S_{mu}	Derivative of f_m by the varactor voltage u_m.
S_{au}	Derivative of f_a by the varactor voltage u_m.
S_{af}	Derivative of f_a by the output frequency f_{mr}.
U	Varactor dc voltage.
u_m	Varactor ac voltage.

I. INTRODUCTION

THE advantage of direct dc/RF conversion in microwave solid-state oscillators is obvious. Just as important are simple low-loss linear FM modulators allowing compact and reliable low-power transmitters or drivers for communication transmitters.

The basic dilemma is to compensate the inherent nonlinearity of the varactor modulator, without strong degradation in efficiency and noise performance. The single-tuned varactor modulator [Fig. 1(a)] with its low degree of freedom allows for a given loaded Q only a compromise between linearity and varactor loss [9], [10]. A summary of analytical results on this circuit is given in Appendix B.

E. D. Reed proposed the inserting of a second resonator between a frequency modulated klystron and its load [1]. By choosing proper couplings and detuning, it is possible over a certain deviation range to compensate the nonlinearity of the klystron's FM characteristic. In a recent paper [2] the application of the coupled resonator linearizing method to a solid-state FM oscillator has been reported, where the first resonator included the varactor and the second the Gunn device [Fig. 1(b)].

In this method fundamental frequency, output coupling, and FM linearizing are to be adjusted by the same circuit parameters. The energy storage in the varactor resonator is determined by the linearity requirements and by the total output power, and is of the same order of magnitude as the energy in the Gunn resonator.

In this report a new linearizing principle, using harmonic tuning, and its application will be presented. After discussing the theoretical background, the nonlinear feedback model of the circuit is developed and a mathematical formulation of the linearity requirements is given.

In Section III the principle is applied to the case of second harmonic tuning. Frequency modulation performance is predicted by analytical and numerical calculations.

Finally, the experimental work, performed with this modulator, is described, emphasizing both circuit and system aspects.

II. THE EFFECT OF HARMONIC TUNING

A. Principle of Linearization, the Feedback Model

The basic idea of the new linearizing techniques is to take advantage of the presence of higher harmonics across the active nonlinear device in the negative resistance FM oscillator.

Manuscript received January 11, 1974; revised June 3, 1974.
The author is with the Systems Research Department, Telefon AB L M Ericsson, Stockholm, Sweden.

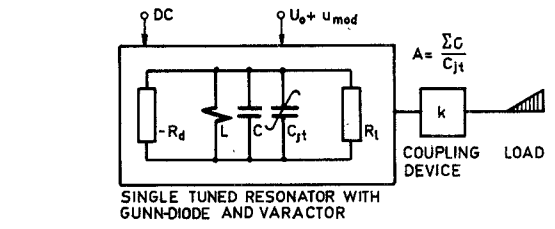

(a)

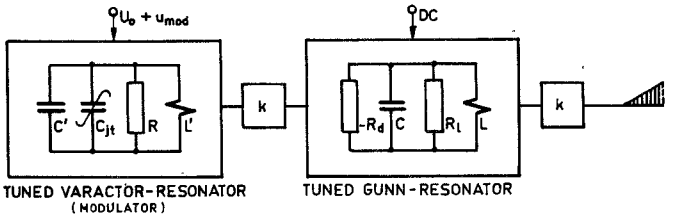

(b)

Fig. 1. Varactor modulated oscillator with one degree of freedom (a) and linearized by a secondary resonator at f_0 (b).

Groskowsky, van der Pol, and others have shown [3]–[5], that these harmonics have a perturbating effect on the oscillation frequency. The ratio between the stationary oscillating frequency (f) and the natural frequency of the resonator circuit (f_0) can be calculated as a function of the harmonic amplitudes (a_n) according to (1).

$$f^2/f_0^2 = \sum_{n=1}^{\infty} a_n^2 / \sum_{n=1}^{\infty} n^2 a_n^2 \tag{1}$$

$$\frac{\Delta f}{f_0} = \frac{f - f_0}{f_0} = -\sum_{n=2}^{\infty} \left(\frac{n^2 - 1}{2}\right) \frac{a_n^2}{a_1^2}. \tag{2}$$

No assumptions have been made on the device characteristic, but the denominator must converge. For weak harmonics $n^2a^2 \ll a_1^2$ the frequency perturbation can be derived in the form of (2). Tuning the resonator (varactor FM) f_0 and f will have the same deviation if the harmonic amplitudes are constant, that is, in the case of broad-band harmonic termination.

But, if at least *one of the harmonics is selectively terminated*, the resulting output frequency deviation ($\Delta f_{mr} = \Delta f$) will differ from the modulator deviation ($\Delta f_m = \Delta f_0$). This is because of the varying amplitude of the selected harmonic component, giving a tuning-dependent frequency perturbation (Δf_a) according to (2). By proper shaping of the transfer function $H(j\omega)$ at the frequency nf [$H(j\omega) = H_n(j\omega)$], the nonlinearity of the original FM characteristic can be eliminated or significantly decreased over a certain deviation range [6], [7].

The principle is shown by the block diagram in Fig. 2 for second harmonic tuning. In our investigations we assume that narrow-band variations of the actual harmonic level are only depending on $H_n(j\omega)$. Frequency perturbation Δf_a is a function of the output frequency deviation so that

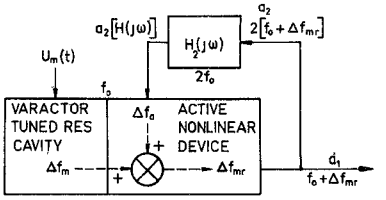

Fig. 2. Principle of compensation. The feedback model.

$$\Delta f_m + \Delta f_a(\Delta f_{mr}) = \Delta f_{mr}. \tag{3}$$

The model makes the understanding and the circuit analysis of the linearized modulator easier and also suggests the application of more general results of nonlinear feedback theory.

The frequency perturbation, as a function of Δf_{mr} will be

$$\frac{\Delta f_a}{f_0} = -\frac{n^2 - 1}{2} \left(\frac{a_n}{a_1}\right)^2 |H_n(j\omega)|^2. \tag{4}$$

B. Analytical Formulation of the Linearity Requirements

To provide good FM performance the variations of the modulator sensitivity within the deviation range must be small. This requirement can be expressed mathematically as constraints on the second and higher derivatives of the modulator output frequency-voltage function or, which is the same, on the first and higher dreivatives of the slope function S.

Varactor FM distortions are dominated by the quadratic term, therefore we prescribe, that the relative harmonic level (a_n/a_1) and the poles of the harmonic transfer function $H_n(j\omega)$ are to be chosen so that the following condition (5) over a certain range of u_m is satisfied

$$\left| \frac{d^2 f_a}{du_m^2} + \frac{d^2 f_m}{du_m^2} \right| \leq \epsilon. \tag{5}$$

A simple case is when requiring the second derivative of the output frequency Δf_{mr} to be zero at $u_m = 0$. This means that the modulator sensitivity has a local minimum at the bias point (Fig. 3).

The derivatives of the modulator output frequency-voltage characteristics are presented in Appendix A. With $\epsilon = 0$ in (5) or with

$$\left. \frac{d^2 f_{mr}}{du_m^2} \right|_0 = 0$$

in (A3) one gets

$$\left. \frac{d^2 f_a}{du_m^2} \right|_0 + \left. \frac{d^2 f_m}{du_m^2} \right|_0 = 0. \tag{6}$$

The same condition will be used in Section III-A, in the analysis of the second harmonic-tuned FM oscillator.

A more severe constraint is requiring an inflection of the modulator sensitivity function at the bias point ($u_m = 0$),

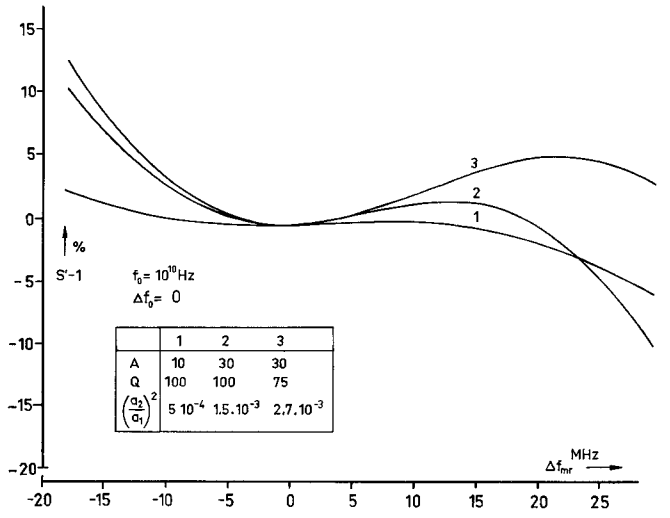

Fig. 3. Normalized modulation sensitivity of linearized oscillator with different optimum conditions.

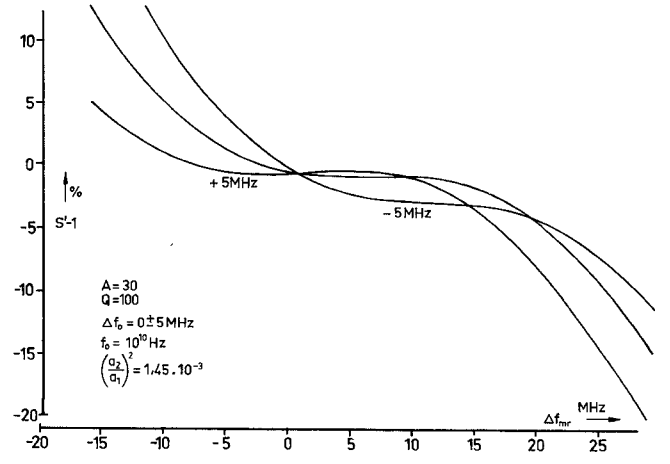

Fig. 4. Normalized modulation sensitivity with the detuning of the second harmonic resonator as parameter.

as in Fig. 4. In this case the quadratic term around the working point can be neglected and the third-order distortion limits the performance. In mathematical terms both the second and the third derivatives of the output frequency are set equal to zero and we get the following system of two equations:

$$\frac{d^2 f_a}{df_{mr}^2}\left(\frac{S_{mu}}{1 - S_{af}}\right)^2 + \frac{d^2 f_m}{du_m^2} = 0 \tag{7}$$

$$\frac{d^3 f_a}{df_{mr}^3}\left(\frac{S_{mu}}{1 - S_{af}}\right)^3 + \frac{d^3 f_m}{du_m^3} = 0. \tag{8}$$

If there is any solution in the deviation range of interest, it will define the relative position of the harmonic transfer function poles with respect to the fundamental frequency and also the necessary harmonic level (a_n/a_1) across the active element. Mathematically, (8) is the consequence of the condition $(d^3 f_{mr}/du_m^3) = 0$ and therefore, the roots of (8) are inflection points of the slope function (df_{mr}/du_m). Nevertheless, the explicit solution of (7) and (8) and the

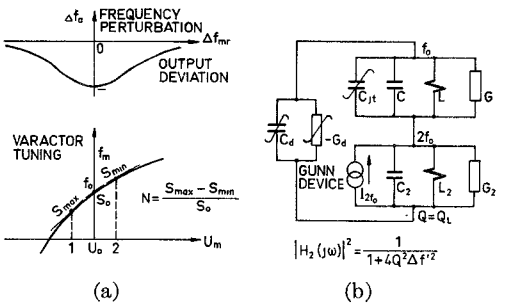

Fig. 5. Circuit diagram (b) and modulation characteristics (a) of FM oscillator with second harmonic tuning.

interpretation of the results can be difficult. One can recall that we are considering the quasi-stationary behavior of the nonlinear feedback model of **Fig. 2.** Thus for a fixed set of circuit parameters, and for an arbitrary sequence of the output $\{f_{mr}\}_1^n$ the corresponding input values $\{u_m\}_1^n$ can be calculated point by point, describing the static modulator characteristic over the range of interest. This numerical procedure does not give the functional relationships necessary to predict and optimize modulator performance in general. On the other hand starting with a parameter set which satisfies (7) the characteristic can be adjusted to fit both (7) and (8). Moreover, the numerical method allows sensitivity analysis over wide deviation ranges.

III. FM OSCILLATOR WITH SECOND HARMONIC TUNING

The parallel-resonator representation of the circuit is shown in Fig. 5(b). The circuit nonlinearities as harmonic power sources are represented by the current generator at $2f_0$. The analysis of this type of nonlinear tuned-circuit model is known from the literature [8]. The relative harmonic level can be calculated if the circuit nonlinearities are given in some explicit form. The frequency perturbation is given by (4)

$$\Delta f_a = -\frac{3}{2}\left(\frac{a_2}{a_1}\right)^2 f_0 \frac{1}{1 + k\Delta f_{mr}^2}, \quad \text{where } k = (2Q/f_0)^2. \tag{9}$$

Fig. 5(a) shows the shape of the frequency deviation caused by the varactor modulator and by the perturbating harmonic content. The quadratic components of f_a and f_m as functions of u_m, respectively, Δf_{mr}, have opposite signs as a basic condition of the compensating effect. Off center frequency, the tuned harmonic circuit may considerably influence the stability of the whole circuit. The problem in its simplest mathematical formulation appears in (A1), Appendix A.

In this paper investigations will be performed on the properties of the modulation sensitivity function assuming a unique and stable oscillatory state of the system. General stability conditions and the dynamic behavior of the frequency feedback system will not be penetrated here.

A. The Required Harmonic Level

If the harmonic transfer function $H_2(j\omega)$ is known, an explicit formula for the second harmonic level can be found, satisfying condition (5). Equation (B7) in Appendix B gives the second derivative of the varactor FM characteristic. The first and second derivatives of the frequency perturbation function are

$$\frac{df_a}{df_{mr}} = S_{af} = \frac{3}{2}\left(\frac{a_2}{a_1}\right)^2 f_0 \frac{2k\Delta f_{mr}}{(1 + k\Delta f_{mr}^2)^2} \tag{10}$$

$$\frac{d^2f_a}{df_{mr}^2} = -\frac{3}{2}\left(\frac{a_2}{a_1}\right)^2 f_0 \frac{6k^2\Delta f_{mr}^2 - 2k}{(1 + k\Delta f_{mr}^2)^3}. \tag{11}$$

For small deviations $S_{af} = 0$ and

$$d^2f_a/df_{mr}^2 = 3(a_2/a_1)^2 f_0 k.$$

Substituting this and (B7) into (7), the relative harmonic level as a function of the circuit parameters n, A, and Q can be expressed as

$$\left(\frac{a_2}{a_1}\right)^2 = \frac{A}{(2Q)^2}\left(\frac{2}{3}\frac{n+1}{n} - \frac{1}{A}\right). \tag{12}$$

If $A \gg 1$ and $n = 0.5$ (12) becomes

$$(a_2/a_1)^2 = A/2Q^2. \tag{13}$$

Fig. 3 shows the normalized modulator sensitivity function, calculated and plotted for different n, A, Q parameter sets. This numerical calculation is based on the nonlinear feedback model shown in Fig. 2 and will be described in detail in the next section.

B. Numerical Optimization

We define, as our purpose, to find the circuit parameters for which the modulation sensitivity is nearly constant around its inflection.

In mathematical terms, both (7) and (8) have to be satisfied. The outline of the numerical computation has already been sketched at the end of Section II-A. The details are summarized in Appendix C. As a result, the modulation sensitivity is plotted, as a function of the output frequency deviation, and normalized to S_0. The same function is displayed by a radio link analyzer, when measuring the differential gain of a frequency modulator.

The harmonic level defined by (12) results in the type of characteristic shown by Fig. 3. However, modifying $(a_2/a_1)^2$ by trial and error, one readily arrives at the optimal shape, shown as the reference characteristics in Figs. 4 and 6. This numerical-graphical method provides a simple means of sensitivity analysis. Investigation of two different variables are shown in Figs. 4 and 6. In the first case Δf_0 has been changed by ± 5 MHz, corresponding to a change of the frequency difference between the fundamental and the harmonic resonators, caused by varying environmental factors as temperature, pushing, pulling, etc. The second example illustrates how modulator performance responds to variations in the relative harmonic level, caused again by external factors (Fig. 6).

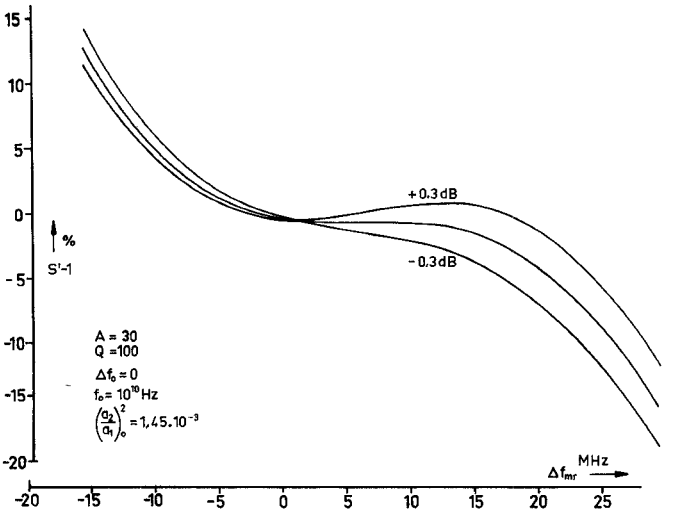

Fig. 6. Normalized modulation sensitivity with the second harmonic level as parameter.

C. Relationship Between Deviation and Nonlinearity

We are considering the optimized cubic-type characteristic (Fig. 4) and will express the maximum frequency deviation for a certain allowed nonlinearity. As a measure of nonlinearity the variation of the normalized slope function is used. Assuming symmetry around the inflection point we define $N/2$ as the normalized, one side deviation from S_0. With (A2) together with the assumptions that $A \gg 1$ and $\Delta f_m = \Delta f_{mr}$ one gets

$$\frac{N}{2} = \frac{\Delta S}{S_0} = \frac{\Delta S_{mu} + \Delta S_{au}}{S_0} = \frac{\Delta S_{mu}}{S_0} + \frac{S_{mu}}{S_0}\frac{S_{af}}{1 - S_{af}}$$

$$= \frac{\Delta S_{mu}}{S_0} + \frac{1 + S_{mu}/S_0}{1 - S_{af}} S_{af} \tag{14}$$

where ΔS_{mu} and S_{af} are given by (B3) and (10), respectively. A closer examination shows, that, if $4Q^2 f_m'^2 \ll 1$ holds, then $1 + (\Delta S_{mu}/S_0)/1 - S_{af} = 1$, and thereby

$$\tfrac{1}{2}N = S_{af} - 2[(n+1)/n]A\Delta f_m'.$$

The series expansion of S_{af} around the inflection point yields for the cubic term of N

$$N = -32[(n+1)/n]AQ^2\Delta f_m'^3. \tag{15}$$

The relative output frequency deviation from the inflection point, resulting in the given nonlinearity, is given by

$$\Delta f_m' = -\left(\frac{1}{32}\frac{n}{n+1}\frac{N}{AQ^2}\right)^{1/3}. \tag{16}$$

Comparison between numerical and analytical results for $n = 0.33$ and $n = 0.45$ verified the validity of the approximative relation (16) within ± 5 percent.

D. Design Aspects

The analysis of the second harmonic-tuned FM oscillator, based on the feedback model in Fig. 2, gave expressions for the required harmonic level (13) and for the maximum frequency deviation, resulting in given nonlinearity (16). These results were then compared with those obtained from numerical simulations of the same model. Consider a microwave circuit configuration which can give the wanted harmonic amplitude behavior. Establishing the equivalence conditions between the two models the microwave circuit parameters can be calculated.

In this section we consider problems around the realization and measurement of some basic parameters. The measurement and control of the relative harmonic level across the active device and the evaluation of second harmonic circuit parameters have to be performed by indirect methods. Thus, because of the nature of the microwave circuitry, Gunn diode parasitics are tuned at the fundamental frequency but not at the harmonics. Furthermore, single-mode wave and impedance concepts cannot be used in waveguide structures because of the possible existence of higher modes at the harmonics.

The second harmonic level can be controlled by the coupling between the active device and the harmonic resonator. The resistive load of the oscillator also affects the value a_2/a_1. In self-limiting negative resistance oscillators the excitation into the nonlinear part of the device characteristics is dependent on the load resistance. The output power of Gunn oscillators, on the other hand shows little load dependence.

The tuned-harmonic linearizing procedure has very little effect on fundamental frequency tuning and output power, in contrast to linearization methods using coupled resonators of the same frequency f_0.

At a prescribed nonlinearity (N) (16) gives a good approximation of the deviation $\Delta f'$ even for roughly estimated n, A, and Q values, because of the cubic root-dependence of this function. The modulator sensitivity function can be investigated over an arbitrary deviation range using the numerical-graphical analysis described previously. Taking different, measured, or estimated values for the temperature dependence of Δf_0 and a_2/a_1, plotted characteristics like those shown by Figs. 4 and 6 will predict modulator performance as a function of temperature.

IV. EXPERIMENTAL WORK

The experimental modulator consists of a waveguide Gunn oscillator (WR 90) deviated by a matched pair of varactors (Fig. 7). The varactors are symmetrically mounted at the front end of the noncontacting, cylindrical, low-pass-type short. The geometric shapes of this end and of the strip connecting the varactors provide broad-band coupling to the resonator. The distance between the virtual short circuit plane and the diode post determines the center frequency of the FM oscillator. Mechanical tuning can be performed by moving the short

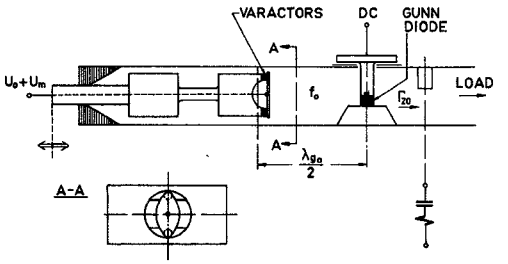

Fig. 7. The experimental waveguide FM oscillator.

assembly along the waveguide axis. A screw across the waveguide establishes the reflection factor Γ_{20} at the second harmonic, which is transformed to the active device and presents the wanted selective termination at $2f_c$. As a consequence of the ambiguity of harmonic impedance calculation and measurement, the parameters of this circuit are experimentally optimized. The successive adjustments of the fundamental and the harmonic frequency circuits converge quickly because of the weak coupling between them.

For the basic modulator/oscillator 100-mW and 250-mW Gunn diodes have been used. All the presented results refer to the 250-mW unit (MA 49159). This circuit has more than 100-MHz electronic tunage range and about 0.4-dB modulator loss. The corresponding-uncompensated-linearity was 15–25 percent at $2\Delta f_m = 8$ MHz$_{pp}$, depending on bias and matching conditions.

The experiments performed with the linearized modulator included linearity, group delay time variation ($\Delta\tau$), noise loading, and FM-noise measurements (Figs. 8 and 9). The noise loading conditions corresponded to those given by CCIR for a 960-channel system and measured values include FM demodulator distortions and baseband noise. FM (thermal) noise was estimated from baseband noise spectrum measurements using identical Gunn oscillators as FM transmitter and receiver LO. The integrated rms noise deviation was about 200 Hz between 5 Hz and 10 kHz, and 1 kHz between 5 Hz and 4 MHz. Experimental FM-oscillator performance is summarized in Table I.

V. CONCLUSIONS

We have shown that the harmonic content of the voltage across the active nonlinear device of a negative-resistance FM oscillator can be used to compensate the nonlinearity of the modulator by selectively terminating at least one of the harmonics. Using van der Pol's expression (1) and the feedback model in Fig. 2, circuit optimization methods could be developed, giving different types of FM characteristics with low static distortion. The detailed analysis of second harmonic tuning gave explicit relations between required modulator performance and circuit parameters.

System-oriented measurements were performed on an experimental 250-mW X-band Gunn-diode FM oscillator. The low static and dynamic intermodulation, low losses, and good noise performance of the new FM oscillator

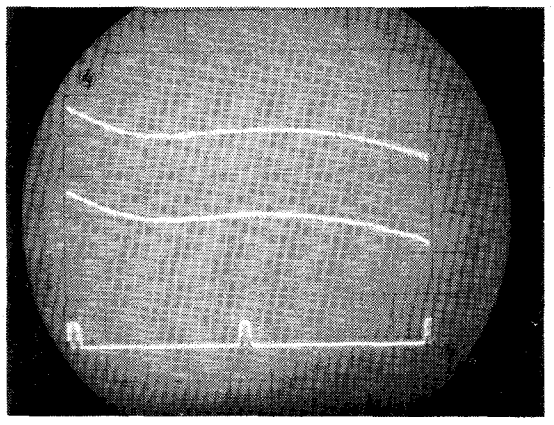

(a)

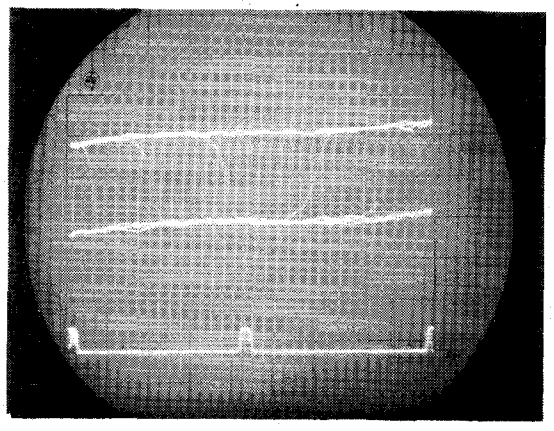

(b)

Fig. 8. Normalized nonlinearity (a) and group delay time variation (b) of the experimental modulator. Frequency markers at ±7 MHz; N = 1 percent and $\Delta\tau$ = 1 ns between parallel tracks.

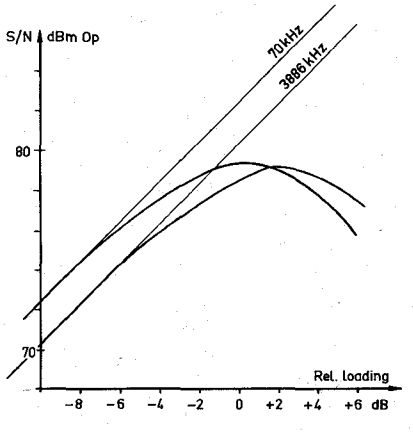

Fig. 9. Noise loading of the experimental modulator, performed without preemphasis.

TABLE I
X BAND FM GUNN OSCILLATOR PERFORMANCE

Output power	250 mW
Modulator losses	0,5 dB (typically 0,4 dB)
Mechanical tuning	0,5 GHz
Linearity	<1% over ± 7 MHz
$\Delta\tau$	<0,5 ns at f_m =.500 kHz
Noise loading	S/N > 76 dB at 0 dB rel. level

allows its application in broad-band radio links satisfying CCIR requirements. It can serve as a single-stage transmitter or being followed by a solid-state amplifier.

APPENDIX A
DERIVATIVES OF THE FREQUENCY-VOLTAGE CHARACTERISTICS

The basic relation between modulator (f_m), perturbation (f_a), and output (Δf_{mr}) frequencies is given by (3). The slope functions, used in the following, are defined, in turn, as $S_{mu} = df_m/du_m$, $S_{af} = df_a/df_{mr}$, and $S_{au} = df_a/du_m$. The first, second, and third derivatives of the output frequency are

$$df_{mr}/du_m = [S_{mu}/(1 - S_{af})] \tag{A1}$$

$$S_{au} = S_{mu}[S_{af}/(1 - S_{af})] \tag{A2}$$

$$\frac{d^2f_{mr}}{du_m^2} = \frac{1}{1 - S_{af}}\left[\frac{d^2f_a}{df_{mr}^2}\left(\frac{S_{mu}}{1 - S_{af}}\right)^2 + \frac{d^2f_m}{du_m^2}\right] \tag{A3}$$

$$\frac{d^3f_{mr}}{du_m^3} = \frac{1}{1 - S_{af}}\left[\frac{d^3f_a}{df_{mr}^3}\left(\frac{S_{mu}}{1 - S_{af}}\right)^3 + 3\,\frac{d^2f_a}{df_{mr}^2} \cdot \frac{d^2f_{mr}}{du_m^2}\left(\frac{S_{af}}{1 - S_{af}}\right) + \frac{d^3f_m}{du_m^3}\right]. \tag{A4}$$

The harmonic transfer function $H_n(j\omega)$ appears in the derivatives d^nf_a/df_{mr}^n.

APPENDIX B
ANALYSIS OF THE SINGLE-TUNED VARACTOR MODULATOR

The circuit diagram of the modulator is shown in Fig. 1. The junction capacitance of the varactor can be expressed as

$$C_j(U_m) = C_j(0)\,(U_m/\phi)^{-n} \tag{B1}$$

where $n = 1/2.2$ for abrupt junction and $n = 1/2.8$ for graded junction. ϕ, the contact potential is a material property, 1.1 for GaAs and 0.5 for Si. We define the nonlinearity, according to Fig. 5(a) as

$$N = (S_{max} - S_{min})/S_0. \tag{B2}$$

The Taylor expansion of the differential sensitivity up to the third term is

$$S_{mu} = df_m/du_m = S_0 + S_1\Delta U_m + S_2\Delta U_m^2 \tag{B3}$$

where $\Delta U_m = U_m - U_0$ and f_m is the voltage-dependent frequency of the FM oscillator. From (B2) and (B3) we get

$$N = -2\Delta U_m(S_1/S_0). \tag{B4}$$

We introduce the ratio between the sum of the resonator capacitances and the transformed junction capacitance of the varactor

$$A = \frac{\sum C}{C_{jt}} = \frac{C + C_{jt}}{C_{jt}}. \tag{B5}$$

The calculation of the coefficients in (B3) gives [9]

$$S_0 = \left.\frac{df_m}{du_m}\right|_{u_0} = -\frac{n}{2} f_0 \frac{1}{A} \cdot \frac{1}{u_0} \tag{B6}$$

$$S_1 = \left.\frac{d^2 f_m}{du_m^2}\right|_{u_0} = -3\frac{S_0^2}{f_0} A \left(\frac{2}{3}\frac{n+1}{n} - \frac{1}{A}\right). \tag{B7}$$

Substituting these equations into (B4), the nonlinearity can be expressed as

$$N = 6\frac{\Delta f_m}{f_0} A \left(\frac{2}{3}\frac{n+1}{n} - \frac{1}{A}\right). \tag{B8}$$

It is easy to see that the "ideal" modulator can be realized by choosing $A = 1$ and $n = 2$. Practical circuits have always $A > 1$, compensated often by the application of hyperabrupt varactors ($n > 2$). Varactor losses, however, limit the possible improvements at microwave frequencies.

EFFICIENCY

We define the resonator $-Q$ with the resonator losses and the load as

$$Q_r = \omega_0 \sum C / G_r$$

the varactor $-Q$ with G_{vt}

$$Q_v = \omega_0 C_{vt} / G_{vt}$$

and the resulting $-Q$ as

$$Q_{rv} = \omega_0 \sum C / (G_r + G_{vt}).$$

The relation between these three Q factors, corresponding to our circuit model is

$$\frac{1}{Q_{rv}} = \frac{1}{Q_r} + \frac{1}{A}\frac{1}{Q_v}. \tag{B9}$$

Assuming optimal loading of the active device, the efficiency of the varactor modulator will be defined as the ratio between the power derived to G_r and the total available power from the diode. The definition yields

$$EF = \frac{Q_{rv}}{Q_r} = 1 - \frac{Q_{rv}}{Q_v}\frac{1}{A} = \frac{1}{1 + (Q_r/Q_v)A^{-1}}. \tag{B10}$$

Fig. 10 gives a graphical presentation of the relation expressed by (B10). Design objectives are Q_{rv} and EF, and at a given varactor quality factor (Q_v) a compromise must be found between them.

It is important to recognize that, according to (B10), realizability requires $A > (Q_{rv}/Q_v)$. This condition appears in Fig. 10 as a vertical asymptote at $(Q_{rv}/Q_v)_k$ to the left of each characteristic having $(Q_{rv}/Q_v)_k$ = constant as parameter.

APPENDIX C
NUMERICAL CALCULATIONS

At a fixed varactor exponent (n), for each characteristic an $\{A,Q\}$ pair is chosen. The second harmonic level, satisfying condition (5), is given by (12). The independent variable is the resulting output frequency deviation, Δf_{mr}. Under the assumptions of Section III-B the frequency perturbation is given by (9). If the harmonic resonator is detuned from $2f_0$ by Δf_0 then $\Delta f = \Delta f_0 + \Delta f_{mr}$ has to replace Δf_{mr}.

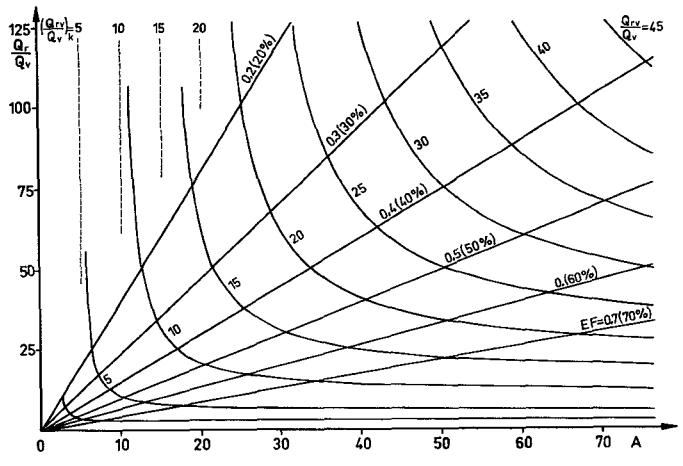

Fig. 10. Circuit quality factors and efficiency of the single-tuned varactor modulator.

The necessary deviation of f_0 caused by the varactor is given by

$$\Delta f_m = \Delta f_{mr} - (\Delta f_a - \Delta f_{a0}) \tag{C1}$$

and using (B1) and the resonance condition the corresponding voltage across the varactor can be calculated as

$$U_m = U_0(A\{[f_0/(f_0 + \Delta f_m)]^2 - 1\} + 1)^{-1/n}. \tag{C2}$$

If the output frequency step Δf_{mr} is held constant, the normalized slope function can be derived by numerical differentiation

$$S_n' = \frac{S_n}{S_0} = \frac{\Delta f_{mr}}{U_{m,n} - U_{m,n-1}} \Big/ \frac{\Delta f_{mr}}{U_1 - U_0} = \frac{\Delta U_0}{\Delta U_{m,n}}. \tag{C3}$$

Finally, $S_n'[\text{percent}] = 100(S_n' - 1)$ is plotted against the output frequency deviation.

ACKNOWLEDGMENT

The author wishes to thank G. Holtzberg for his help in performing the experiments, to G. Gobl for his valuable discussions during the work, and to Prof. G. Hellgren for his important comments on the manuscript.

REFERENCES

[1] E. D. Reed, "A coupled resonator reflex klystron," *Bell Syst. Tech. J.*, May 1953.
[2] T. Yamashita and M. Okubo, "Frequency modulator using solid device oscillator and varactor," *Fujitsu Sci. Tech. J.*, vol. 7, 1971.
[3] J. Groskowski, "The interdependence of frequency variation and harmonic content and the problem of constant-frequency oscillators," *Proc. IRE*, July 1933.
[4] B. van der Pol, "The nonlinear theory of electric oscillations," *Proc. IRE*, Sept. 1934.
[5] J. P. Quine, "A generalized locking equation for oscillators," *IEEE Trans. Microwave Theory Tech.*, vol. MTT-20, pp. 418–420, June 1972.
[6] G. Endersz, "High-linearity FM Gunn oscillator," presented at the 1973 European Microwave Conference.

[7] "Circuit arrangement to improve the linearity of an angle-modulated oscillator," Swedish Patent Application, No. 73/089062.
[8] P. Penfield and R. P. Rafuse, *Varactor Applications*. Cambridge, Mass.: M.I.T. Press, 1962.
[9] G. Endersz, Memorandum, L M Ericsson, 7546/Ue 2028, 1972.
[10] I. Török, M.S. thesis, Technical University of Budapest, Budapest, Hungary, 1966.

Gunn-Effect Amplifiers for Microwave Communication Systems in *X*, *Ku*, and *Ka* Bands

J. G. DE KONING, MEMBER, IEEE, R. E. GOLDWASSER, R. J. HAMILTON, JR., MEMBER, IEEE, AND F. E. ROSZTOCZY

***Abstract*—This paper describes the design and performance of small-signal stable multistage Gunn-effect reflection-type amplifiers for communication systems in *X*, *Ku*, and *Ka* bands. A single-stage design approach is developed, based on measured small-signal *Z* parameters of the Gunn diodes. This technique is then applied to a microstrip medium at lower frequencies (*X* and *Ku* bands) and to a coax/waveguide hybrid structure at *Ka* band. Performance of a two-stage amplifier is described in the bands 11.7 to 12.2 GHz and 14.0 to 14.5 GHz. In high *Ka* band, performance of both a two- and a four-stage amplifier is presented.**

I. INTRODUCTION

EARLY experiments with low n_0L product ($n_0L < 5 \times 10^{11}$ cm^{-2}) GaAs Gunn devices resulted in low-power narrow-band reflection amplification at microwave and millimeter wave frequencies [1], [2]. Since the first observation of the stabilization of highly doped Gunn devices [3], wide-band Gunn-effect amplifier prototypes in *C*, *X*, and *Ku* band have been built [4]–[8].

Multistage Gunn-effect amplifiers for FM–CW communication systems have been reported, and 1 W at 30 dB gain in *X* band and 0.5 W in *Ku* band have been achieved [9]. These waveguide cavity amplifiers exhibited less than 350-MHz bandwidth, time-delay variations of 5 ns over 200 MHz in *X* band, and considerable gain expansion. Low-power narrow-band (<0.2 GHz) millimeter wave amplification at 34 GHz has been reported using supercritical GaAs and InP devices [10], [11]. Recently, a GaAs Gunn-effect amplifier with 110-mW saturated power output at 35 GHz was described [12]. The single-stage amplifier had a gain of 13 dB and a 3-GHz 3-dB bandwidth.

The objective of this paper is to describe recent advances in Gunn-effect amplifiers designed for microwave communication systems at frequencies ranging from *X* to *Ka* band. Particular attention has been given to achieve minimal variations of gain and phase, intermodulation distortion, and AM–PM conversion. The physics and the impedance characteristics of Gunn diodes from *C* to *Ka* band are discussed, followed by a description of generalized single-stage amplifier design approach. The actual physical design of certain multistage communication amplifiers in *X*, *Ku*, and *Ka* bands will be described.

Manuscript received February 2, 1974; revised June 16, 1974.
The authors are with Varian Associates, Palo Alto, Calif. 94303.

II. GUNN DIODE CHARACTERISTICS AND DISCUSSION OF IMPORTANT PARAMETERS

At sufficiently high electric fields, GaAs exhibits external negative resistance which is caused by a local negative differential mobility inside the crystal. This negative differential mobility can lead to a variety of external appearances, one of which is the stable negative resistance mode.

In the stable negative resistance mode, the diode exhibits an RF impedance with a negative real part for frequencies close to the transit time frequency. The frequency range over which negative resistance is observed is of the order of 1 octave. A stable Gunn diode can be utilized to form an oscillator or a stable reflection amplifier, depending upon the circuit configuration.

In general, the diode parameters required for optimization of power, bandwidth, noise, and stability in an amplifier are very similar to those required for a wide-band oscillator with a similar output power and efficiency. The same diode parameters which lead to wide-band tunability also lead toward stability. Since stability in a realizable circuit is the first criterion, one designs to achieve that characteristic. Generally, n_0L products less than 2×10^{12} cm^{-2} and flat, uniform doping profiles throughout the active layer are preferred.

The package parameters are of critical importance. A micropill package with ceramic dimensions of 0.030 in outer diameter and 0.012 in height has been utilized for the